

Supporting Information

Fluorinated Oligothiophene Donor for High-Performance Nonfullerene Organic Photovoltaics

Tongle Xu,^{‡,a,b} Yuying Chang,^{‡,a} Cenqi Yan,^c Qianguang Yang,^a Zhipeng Kan,^{*a} Ranbir Singh,^{*d} Manish Kumar,^e Gang Li,^c Shirong Lu,^a and Tainan Duan^{*a}

^a *Chongqing Institute of Green and Intelligent Technology, Chinese Academy of Sciences, Chongqing, 400714, China*

^b *University of Chinese Academy of Sciences, Beijing 100049, China*

^c *Department of Electronic and Information Engineering, The Hong Kong Polytechnic University, Hong Hum, Kowloon, Hong Kong, China.*

^d *Department of Energy & Materials Engineering, Dongguk University, Seoul, 100-715, Republic of Korea*

^e *Pohang Accelerator Laboratory, POSTECH, Pohang 37673, South Korea*

Content:

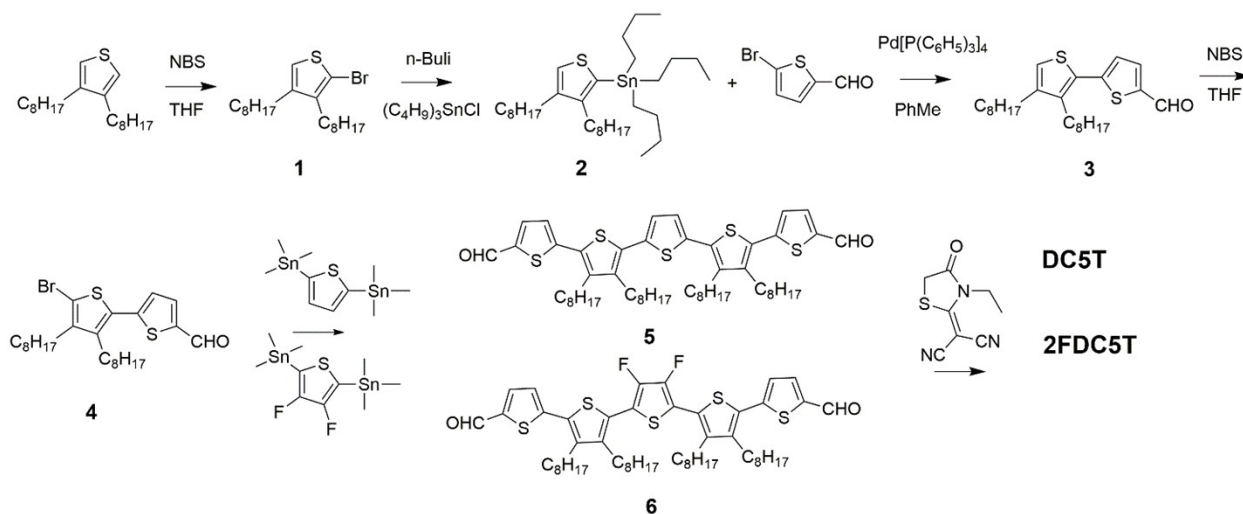
1. General Experimental Details	3
2. Synthetic Protocols and Characterizations	4
3. UV-Vis Absorption Spectra	10
4. Cyclic voltammogram.....	11
5. Differential Scanning Calorimetry (DSC) Measurements	12
6. Device Fabrication.....	13
7. Measurements and Characterizations.....	14
8. The space charge limited current (SCLC) Measurement.....	15
9. Atomic Force Microscopy (AFM) Imaging of as cast	16
10. Transmission Electron Microscopy (TEM) Characterization of as cast films.....	17
11. GIWAXS Characterization.....	18
12. Different processing conditions in optimizing PCE.....	20
13. Solution NMR Spectra	23
14. References.....	39

1. General Experimental Details

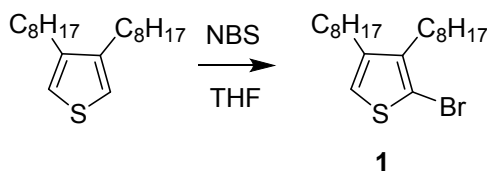
Instrument: ^1H NMR, ^{13}C NMR and ^{19}F NMR spectra were obtained on an AVANCE500 nuclear magnetic resonance (NMR) spectroscope. UV-vis absorption spectra were recorded on a Perkin Eimer Lambda 365 spectrophotometer. Thermo gravimetric analysis (TGA) was carried out on a WCT-2 thermal balance under protection of nitrogen at a heating rate of $10^\circ\text{C}/\text{min}$. Cyclic voltammetry (CV) was done on a CHI600E electrochemical workstation with Pt disk, Pt plate, and standard calomel electrode (SCE) as working electrode, counter electrode, and reference electrode, respectively, in a 0.1 mol/L tetrabutylammoniumhexafluorophosphate (Bu_4NPF_6) CH_2Cl_2 solution. The CV curves were recorded versus the potential of SCE, which was calibrated by the ferrocene-ferrocenium (Fc/Fc^+) redox couple (4.8 eV below the vacuum level). Topographic images of the films were obtained on a Veeco Multi Mode atomic force microscopy (AFM) in the tapping mode using an etched silicon cantilever at a nominal load of $\sim 2\text{nN}$, and the scanning rate for a $10\ \mu\text{m} \times 10\ \mu\text{m}$ image size was 1.5 Hz. In order to investigate the phase distribution of the active layer by testing the Transmission Electron Microscope (TEM) by Talos F200S.

Materials: All reagents and solvents, unless otherwise specified, were purchased from Energy Chemical, Tansoole, Suna Tech, Aldrich and JiangSu GE-Chem Biotech., Ltd, without further purification. 3,4-dioctylthiophene was synthesized according to the previous literature report.^[1] **IDIC-4F** was purchased from Solarmer Energy Inc.

2. Synthetic Protocols and Characterizations

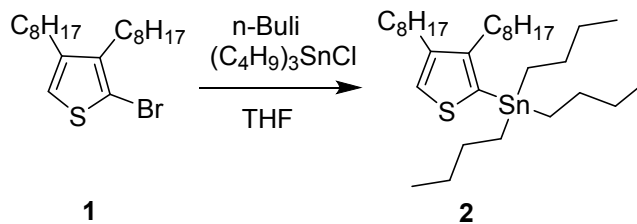


Scheme S1. Synthesis of the donors **DC5T** and **2FDC5T**.



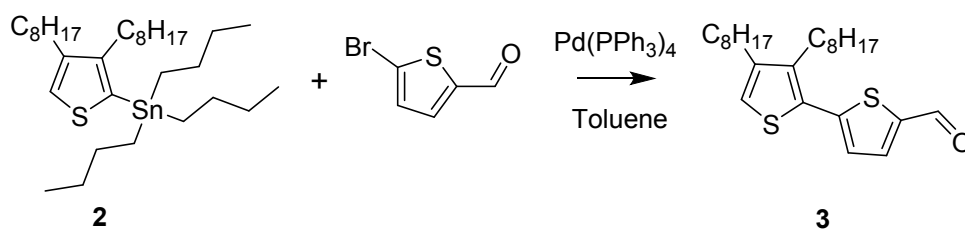
2-bromo-3,4-dioctylthiophene (1)

3,4-dioctylthiophene (1.85 g, 6 mmol) in dry THF (25 ml) was cooled to 0 °C in the dark, N-Bromosuccinimide (NBS 1.067 g, 6 mmol) was added slowly in five minutes. The reaction mixture was warmed to room temperature and stirred for another 3 h. Subsequently, the reaction mixture was quenched by the addition of 20 mL distilled water, and then the mixture was extracted by ethyl acetate (EA). Finally, the combined organic phase was dried with anhydrous MgSO_4 and concentrated to obtain a yellow viscous crude product. The residue was purified by column chromatography on silica gel hexane to give **1** (1.85 g, 80.11%). ^1H NMR (400 MHz, CDCl_3) δ 6.83 (s, 1H), 2.60-2.40 (m, 4H), 1.60-1.45(m, 4H), 1.40-1.25 (m, 20H), 0.91 – 0.86 (m, 6H). ^{13}C NMR (101 MHz, CDCl_3) δ 136.84, 135.87, 114.76, 104.00, 26.73, 24.51, 24.46, 24.35, 24.31, 24.21, 24.17, 24.09, 22.95, 17.51, 8.93.



Tributyl(3,4-dioctylthiophen-2-yl)stannane (**2**)

Compound **1** (1.85 g, 4.8 mmol) in dry THF (20 ml) was cooled to $-78\text{ }^{\circ}\text{C}$ under the protection of argon, and a solution of n-Buli (2.02 ml, 2.5 M in THF, 5.04 mmol) was added dropwise with stirring. The reaction mixture was stirred for 1 h under $-78\text{ }^{\circ}\text{C}$. Next, Tri-n-butyltin chloride (1.875 g, 5.76 mmol) was added in one portion. The reaction mixture was warmed to room temperature and stirred for another 6 h. Subsequently, the reaction mixture was quenched by the addition of 20 mL distilled water, and then the mixture was extracted by EA. Finally, the combined organic phase was dried with anhydrous MgSO_4 and concentrated to obtain a yellow viscous crude product. The residue was used in the next step without the need for further purification.

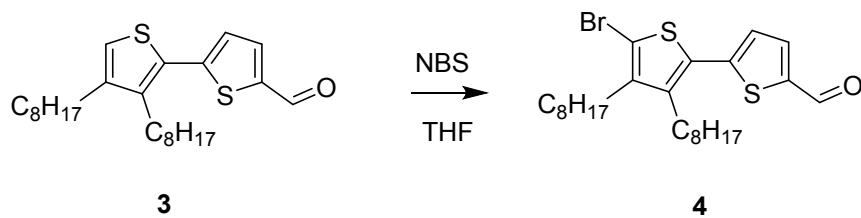


3',4'-dioctyl-[2,2'-bithiophene]-5-carbaldehyde (**3**).

In a pre-dried Schlenk tube, **2** (2.6 g, 4.3 mmol), 5-bromothiophene-2-carbaldehyde (0.742 g, 3.9 mmol), and $\text{Pd}(\text{PPh}_3)_4$ (460.8 mg, 0.43 mmol) were dissolved with degassed toluene (50 mL). The mixture was heated at $110\text{ }^{\circ}\text{C}$ for 24 h. The reaction mixture was allowed to cool down to room temperature, extracted with EA (2×30 mL), dried over Na_2SO_4 , and then concentrated under reduced pressure. The residue

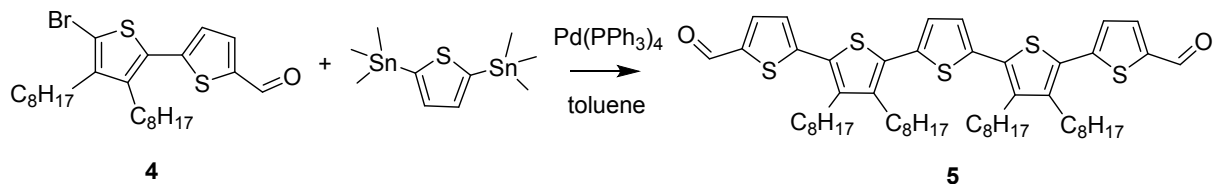
was purified by column chromatography on silica gel hexane/ethyl acetate (50: 1) to give 3 (1.47g, 90%).

^1H NMR (600 MHz, CDCl_3) δ 9.87 (s, 1H), 7.69 (d, $J = 4.2$ Hz, 1H), 7.20 (d, $J = 4.2$ Hz, 1H), 6.96 (s, 1H), 2.77 – 2.70 (t, $J = 8.4$ Hz, 2H), 2.55 – 2.48 (t, $J = 7.8$ Hz, 2H), 1.70-1.60 (m, 2H), 1.56 – 1.50 (m, 2H), 1.43 – 1.38 (m, 4H), 1.35 – 1.25 (m, 16H), 0.96 – 0.81 (m, 6H). ^{13}C NMR (151 MHz, CDCl_3) δ 182.72, 147.64, 144.54, 142.18, 140.78, 136.56, 130.01, 126.24, 121.27, 31.89, 31.87, 30.19, 29.83, 29.74, 29.59, 29.48, 29.31, 29.27, 29.23, 29.23, 29.15, 29.15, 27.92, 22.68, 14.09.



5'-bromo-3',4'-dioctyl-[2,2'-bithiophene]-5-carbaldehyde (4).

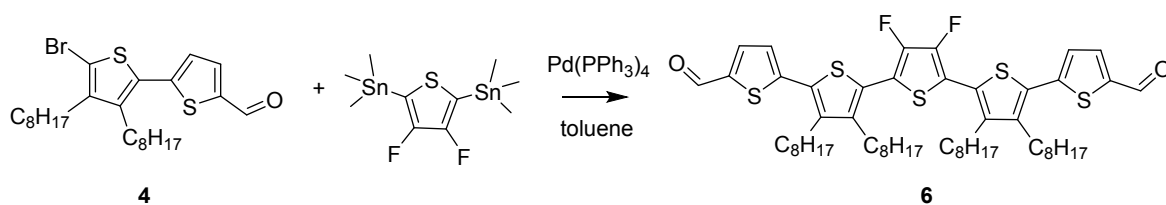
Compound 2 (1.84 g, 4.40 mmol) in dry THF (25 ml) was cooled to 0 °C in the dark, NBS was added slowly in five minutes, The reaction mixture was warmed to room temperature and stirred for another 3 h. Subsequently, the reaction mixture was quenched by the addition of 20 mL distilled water, and then the mixture was extracted by ethyl acetate. Finally, the combined organic phase was dried with anhydrous MgSO_4 and concentrated to obtain a yellow viscous crude product. The residue was purified by column chromatography on silica gel hexane/ethyl acetate (50: 1) to give 4 (2.07 g, 95%). ^1H NMR (600 MHz, CDCl_3) δ 9.88 (s, 1H), 9.88 (s, 1H), 7.68 (d, $J = 3.6$ Hz, 1H), 7.15 (d, $J = 3.6$ Hz, 1H), 2.75 – 2.71 (t, $J = 7.8$ Hz, 2H), 2.56 – 2.52 (t, $J = 8.4$ Hz, 2H), 1.52 (m, 4H), 1.29 (m, 20H), 0.88 (m, 6H). ^{13}C NMR (151 MHz, CDCl_3) δ 182.52, 145.70, 143.39, 142.58, 141.10, 136.58, 130.06, 126.33, 111.17, 31.88, 31.87, 31.84, 30.46, 29.75, 29.69, 29.57, 29.35, 29.32, 29.24, 29.23, 29.19, 29.14, 28.68, 22.67, 14.08.



3',3''',4',4'''-tetraoctyl-[2,2':5',2'':5'',2''':5''',2''''-quinquethiophene]-5,5''''-dicarbaldehyde (5)

In a pre-dried Schlenk tube, **3** (1.25 g, 2.52 mmol), 2,5-bis(trimethylstannyl)thiophene (0.43 g, 1.05 mmol), and Pd(PPh₃)₄ (115.2 mg, 0.10 mmol) were dissolved with degassed toluene (50 mL). The mixture was heated at 110 °C for 24 h. The reaction mixture was allowed to cool down to room temperature, the organic layer was washed with brine, extracted with CH₂Cl₂ (3×40 mL), dried over Na₂SO₄, and then concentrated under reduced pressure. The crude product was purified by column chromatography over SiO₂ using hexanes/CH₂Cl₂ (1:2) as the eluent. The solvent was removed by rotary evaporation, affording compound **4** as a orange solid.(846.8 mg, 88%).

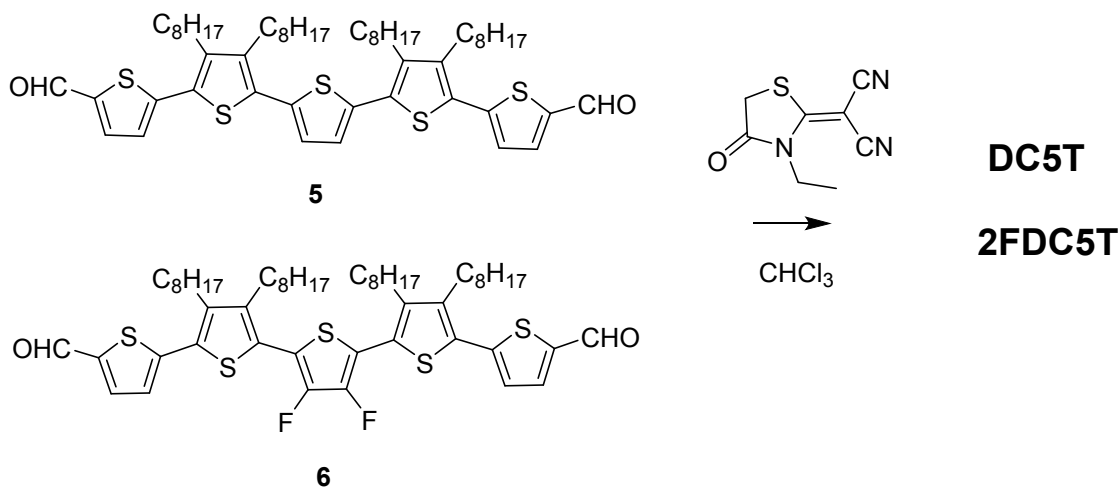
¹H NMR (600 MHz, CDCl₃) δ 9.98 (s, 2H), 7.71 (d, *J* = 3.6 Hz, 2H), 7.24 (d, *J* = 3.6 Hz, 2H), 7.14 (s, 2H), 2.82 – 2.71 (m, 8H), 1.59 – 1.54 (m, 10H), 1.45 – 1.43 (m, 10H), 1.34 – 1.28 (m, 28H), 0.88 (m, 1H). ¹³C NMR (151 MHz, CDCl₃) δ 182.46, 146.30, 142.69, 142.31, 140.90, 136.63, 136.00, 131.88, 129.02, 126.60, 126.16, 31.89, 31.86, 31.86, 30.68, 30.44, 29.91, 29.90, 29.29, 29.27, 29.27, 29.22, 29.22, 28.42, 28.23, 22.67, 14.06.



3'',4''-difluoro-3',3''',4',4'''-tetraoctyl-[2,2':5',2'':5'',2''':5''',2''''-quinquethiophene]-5,5''''-dicarbaldehyde(6)

In a pre-dried Schlenk tube, **3** (0.40 g, 0.81 mmol), (3,4-difluorothiophene-2,5-diyl)bis(trimethylstannane) (0.150 g, 0.336 mmol), and Pd(PPh₃)₄ (60.2 mg, 0.05 mmol) were dissolved with degassed toluene (50 mL). The mixture was heated at 110 °C for 24 h. The reaction mixture was allowed to cool down to room temperature, the organic layer was washed with brine, extracted with CH₂Cl₂ (3×40 mL), dried over Na₂SO₄, and then concentrated under reduced pressure. The crude product was purified by column chromatography over SiO₂ using hexanes/CH₂Cl₂ (1:2) as the eluent. The solvent was removed by rotary evaporation, affording compound **4** as a orange solid.(270.5 mg, 84%).

¹H NMR (600 MHz, CDCl₃) δ 9.90 (s, 2H), 7.72 (d, *J* = 3.9 Hz, 2H), 7.26 (d, *J* = 3.9 Hz, 2H), 2.80 – 2.76 (m, 4H), 2.70 – 2.66 (m, 4H), 1.63 – 1.49 (m, 10H), 1.46 – 1.39 (m, 8H), 1.28 (m, 30H), 0.90 – 0.86 (m, 12H). ¹³C NMR (151 MHz, CDCl₃) δ 182.52, 165.94, 145.71, 143.62, 142.85, 142.70, 142.56, 142.08, 140.94, 140.80, 136.56, 134.28, 131.50, 129.48, 126.63, 125.24, 113.06, 67.79, 38.96, 31.87, 31.85, 30.61, 30.53, 30.48, 29.87, 29.84, 29.69, 29.65, 29.25, 29.24, 29.23, 29.21, 29.00, 28.31, 28.28, 23.98, 22.96, 22.66, 14.07, 11.08. ¹⁹F NMR (565 MHz, CDCl₃) δ -131.68 (s).



General procedure for the preparation of the molecular donors DC5T and 2FDC5T:

Compound **4** or **5** (1.0 equiv.) was dissolved in a dry chloroform (10 mL) and few drops of Triethylamine was added under nitrogen. Then, 2-(3-ethyl-4-oxothiazolidin-2-ylidene)malononitrile((10.0 equiv.) was added and resulting solution was heated to reflux and stirred for 12 h. The reaction mixture was cooled down to room temperature, poured into methanol. The precipitate was filtered and washed several times with methanol. After purified by silica gel column chromatography (eluent: chloroform/hexanes (4 :1), the desired dark black solids were obtained.

DC5T(320 mg, 93%) ^1H NMR (600 MHz, CDCl_3) δ 8.05 (s, 2H), 7.44 (d, $J = 4.0$ Hz, 2H), 7.26 (d, $J = 4.0$ Hz, 2H), 7.16 (s, 2H), 4.34 – 4.30 (m, 4H), 2.81 – 2.74 (m, 8H), 1.62 – 1.54 (m, 10H), 1.46 – 1.40 (m, 10H), 1.32-1.26 (m, 34H), 0.92-0.86 (m, 12H). ^{13}C NMR (151 MHz, CDCl_3) δ 165.85, 165.30, 145.63, 142.87, 141.05, 136.01, 135.83, 135.65, 132.22, 128.77, 128.49, 126.90, 126.73, 113.54, 113.01, 112.24, 55.87, 40.65, 31.89, 30.66, 30.41, 30.33, 29.91, 29.87, 29.68, 29.31, 29.28, 29.17, 28.62, 28.26, 22.67, 14.16, 14.08, 14.08. MS (MALDI) m/z calcd. for $\text{C}_{70}\text{H}_{86}\text{N}_6\text{O}_2\text{S}_7$ $[\text{M}]^+$: 1267.9180, found 1267.49403.

2FDC5T (230 mg, 91%) ^1H NMR (600 MHz, CDCl_3) δ 8.06 (s, 2H), 7.45 (d, $J = 4.0$ Hz, 2H), 7.28 (d, $J = 4.0$ Hz, 2H), 4.33 (m, 4H), 2.82 – 2.77 (m, 4H), 2.72 – 2.68 (m, 4H), 1.61 – 1.54 (m, 10H), 1.44-1.39 (m, 10H), 1.35-1.25 (m, 32H), 0.90 – 0.86 (m, 12H). ^{13}C NMR (151 MHz, CDCl_3) δ 165.82, 165.22, 144.87, 143.70, 142.73, 142.56, 142.21, 140.97, 140.78, 136.37, 135.45, 131.23, 128.36, 127.43, 125.50, 114.01, 113.10, 113.03, 112.94, 112.17, 56.06, 40.68, 31.88, 31.87, 30.53, 30.46, 29.85, 29.25, 29.23, 29.16, 28.47, 28.34, 22.68, 22.66, 14.16, 14.09, 14.07. ^{19}F NMR (565 MHz, CDCl_3) δ -131.32 (s). MS (MALDI) m/z calcd. for $\text{C}_{70}\text{H}_{84}\text{F}_2\text{N}_6\text{O}_2\text{S}_7$ $[\text{M}]^+$: 1302.4669, found 1302.47255.

3. UV-Vis Absorption Spectra

UV-Vis absorption spectra of **DC5T**, **2FDC5T** and **IDIC-4F** were recorded on PerkinElmer LAMBDA 365 UV-Vis spectrophotometer.

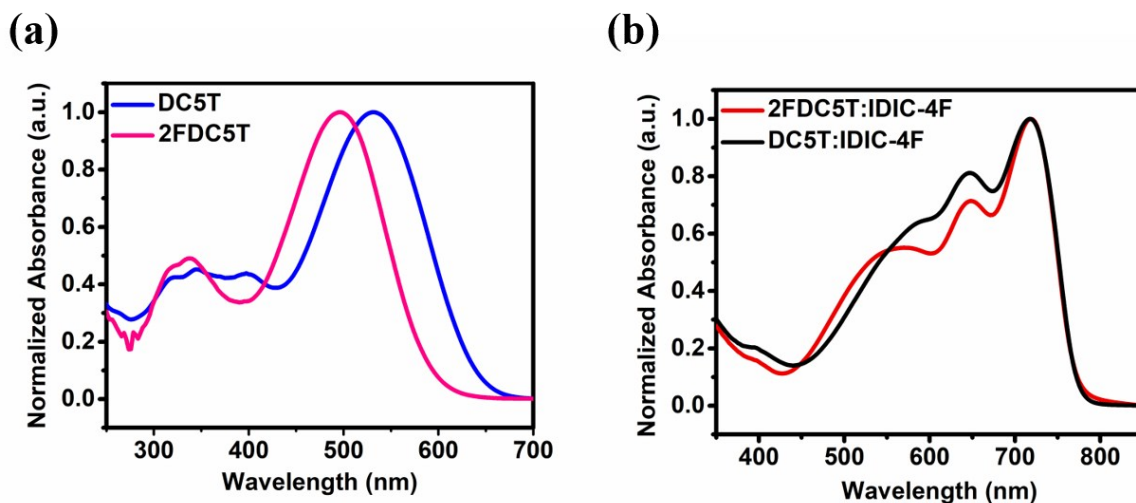


Figure S1. (a) Normalized solution UV-vis absorption spectra of the neat components **DC5T** and **2FDC5T**. (b) Normalized blend-film UV-vis absorption spectra of **2FDC5T:IDIC-4F** and **DC5T:IDIC-4F**.

4. Cyclic voltammograms

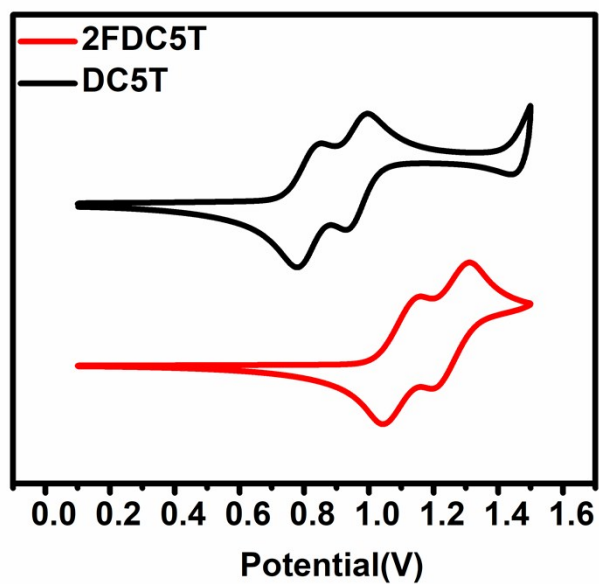


Figure S2. Cyclic voltammograms (positive scan) of **DC5T** and **2FDC5T** in 0.1 mol L⁻¹ Bu₄NPF₆ dichloromethane solutions.

5. Differential Scanning Calorimetry (DSC) Measurements

Differential Scanning Calorimetry (DSC) measurements were performed on a Mettler-Toledo TGA/DSC 3+ analyzer under a nitrogen atmosphere, using aluminum crucibles.

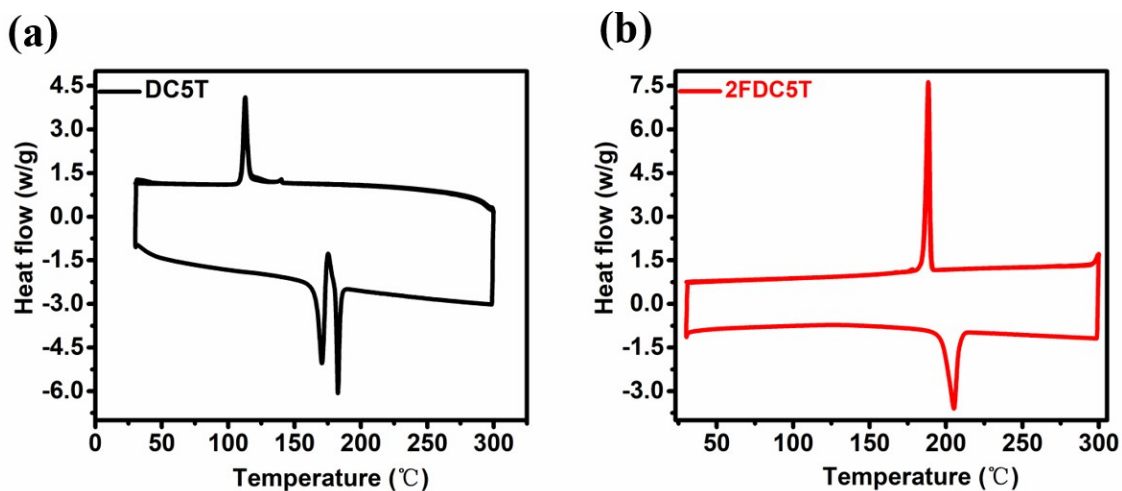


Figure S3. DSC traces of (a) **2FDC5T** and (b) **DC5T**. Analyses carried out with a scan rate of 10°C/min between 30°C and 300°C. **2FDC5T** shows an apparent phase transition around 204°C, **DC5T** shows an apparent phase transition around 170°C and 184°C, suggesting a melt transition in light of the presence of a first order solidification peak on the cooling scan.

6. Device Fabrication

The device structures were ITO/PEDOT:PSS/ active layer/Phen-NaDPO /Ag. The organic solar cell was fabricated on a glass substrate, and tin-substituted indium oxide (ITO) (device area: 0.11 cm²) was patterned on the surface. It was then placed in a beaker containing deionized water and detergent, and the beaker was immersed in an ultrasonic bath for 15 minutes to remove organic residues. The samples were rinsed in flowing deionized water for 5 minutes and then sonicated for 15 minutes in a continuous bath of deionized water, acetone and isopropanol acetate. Next, the substrate was purged with nitrogen. It was exposed to a UV-ozone plasma for 15 minutes. PEDOT:PSS (~30 nm) was spin-coated onto the UV-treated substrate, and then the substrate was placed on a hot plate at 160 °C for 20 minutes, and then the substrate was then transferred to a glove box for active layer deposition.

All solutions were prepared in a donor (**DC5T** or **2FDC5T**) and acceptor **IDIC-4F** glove box; As described above, the small molecule donors **DC5T** and **2FDC5T** were synthesized. The optimized device was obtained by dissolving **DC5T**, **2FDC5T** and **IDIC-4F** in chloroform (CF) at a D/A ratio of 1:1 (wt/wt). The total concentration is 18 mg/ml. Note: The prepared solution was stirred at room temperature overnight and then spin coated onto a PEDOT:PSS substrate. The active layer was spin-coated at an optimum speed of 3000-4000 rpm for 30 s to form a film of 90 to 110 nm. Then, **DC5T** was thermally annealed (the substrate was placed on a hot plate at 130 °C), and **2FDC5T** was subjected to thermal annealing at 110 °C and then solvent-annealed with CF.

Then, Phen-NaDPO was applied as an electron transport layer at 2000 rpm for 30 s to the uppermost layer of the apparatus. Finally, the substrate was evacuated at a pressure of 3×10^{-4} Pa, and then the Ag layer (100 nm) was thermally evaporated onto the active layer. The shadow masks were used to ensure the effective area of the device (0.11 cm²).

7. Measurements and Characterizations

The current density-voltage ($J-V$) curve of the photovoltaic devices were measured in air using a Keithley 2400 source meter, under AM 1.5G (100 mW cm⁻²) using a solar simulator. The external quantum efficiency (EQE) was performed using IPCE equipment (Zolix Instruments, Inc, Solar Cell Scan 100).

8. The space charge limited current (SCLC) Measurement

The SCLC mobility were measured of active layer using a diode configuration by fitting the dark current to the space-charge-limited current (SCLC) model. The specific device structures were the Glass/ITO/PEDOT:PSS/active layer/MoO₃/Ag for the only hole and the Glass/ITO/ZnO/Phen-NaDPO/active layer/Phen-NaDPO/Ag for the only electron in the range of -0.5-5 V. The SCLC is described by:

$$J = \frac{9\varepsilon_0\varepsilon_r\mu_0V^2}{8L^3} \exp\left[0.89\beta\sqrt{\frac{V}{L}}\right]$$

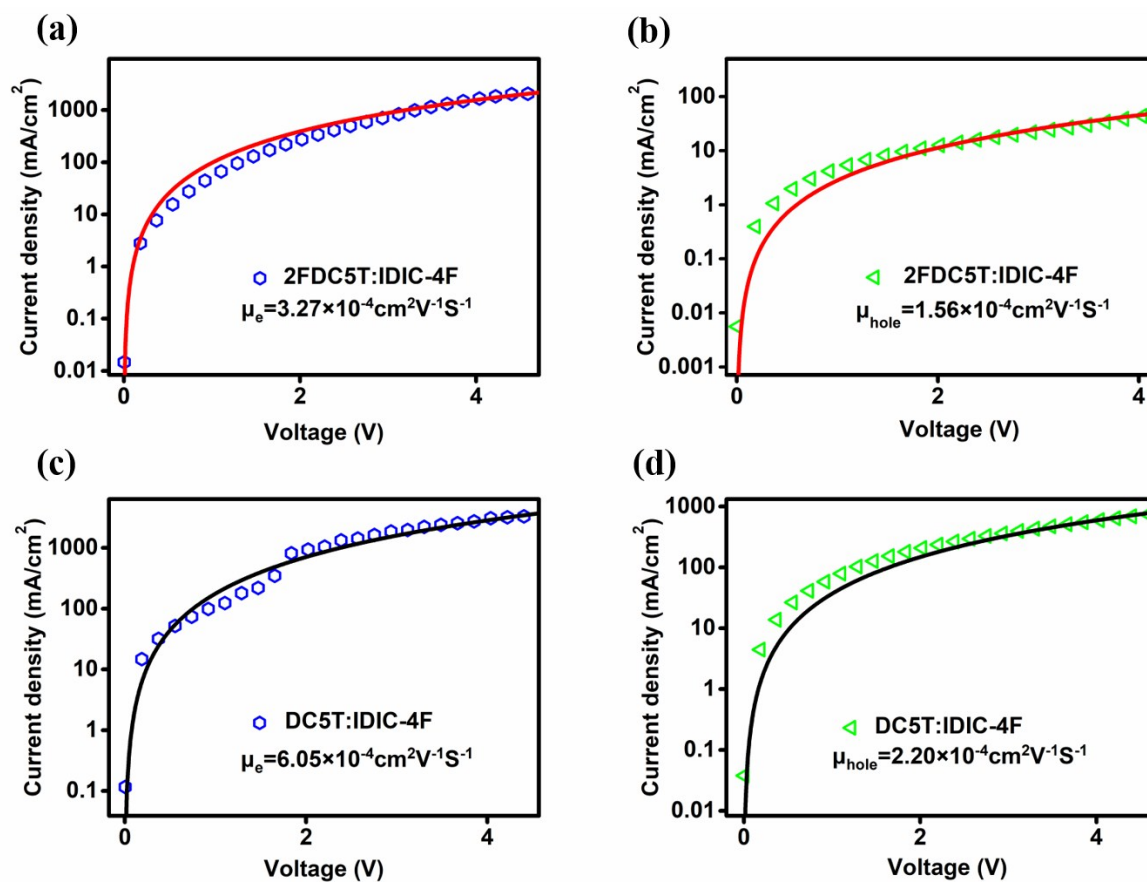


Figure S4. SCLC data for (a), (c) electron-only and (b), (d) hole-only devices fabricated by **2FDC5T:IDIC-4F** and **DC5T:IDIC-4F** respectively.

9. Atomic Force Microscopy (AFM) Imaging of as cast films

A Dimension Icon atomic force microscope (AFM) from Bruker was used to image the active layers in tapping mode (heights and phase images are represented below).

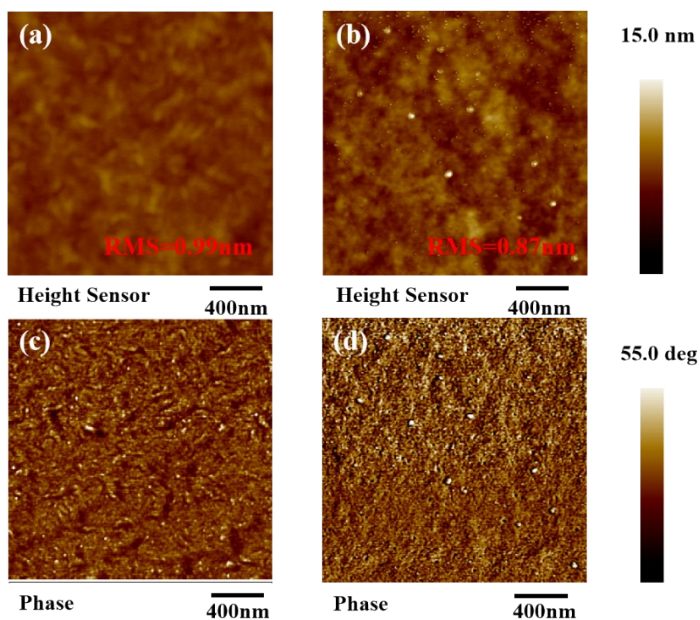


Figure S5. Topography and phase images of as cast thin films with CF. Topography images of (a) DC5T:IDIC-4F; (b) 2FDC5T:IDIC-4F. Phase images of (c) (d) corresponds to Topography images (a) (b), respectively. Scale bar is 400 nm.

10. Transmission Electron Microscopy (TEM) Characterization of as cast films

Films were spun-cast on PEDOT:PSS-coated glass substrates. The **DC5T:IDIC-4F** and **2FDC5T:IDIC-4F** BHJ films were floated off the substrates in deionized water and collected on lacey carbon coated TEM grids (Electron Microscopy Sciences). TEM studies were performed a Thermo Fischer (former FEI) Titan Titan 80-300 TEM equipped with an electron monochromator and a Gatan Imaging Filter (GIF) Quantum 966.

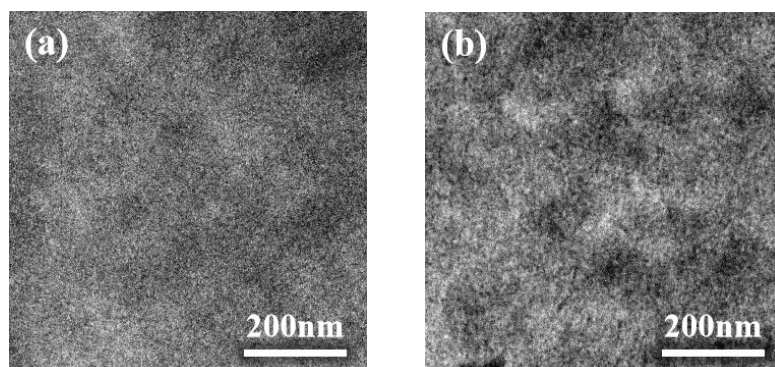


Figure S6. TEM images of the as cast films (a) **DC5T:IDIC-4F**, (b) **2FDC5T:IDIC-4F**, Scale bar is 200 nm.

11. GIWAXS Characterization

Grazing-Incidence wide-angle X-ray scattering (GIWAXS) measurements were performed at 5A beamline of the Pohang Light Source II (PLS-II) in Korea. The GIWAX images were recorded with X-rays of 11.57 keV ($\lambda=1.0716\text{\AA}$) at 0.13 incidence angle.

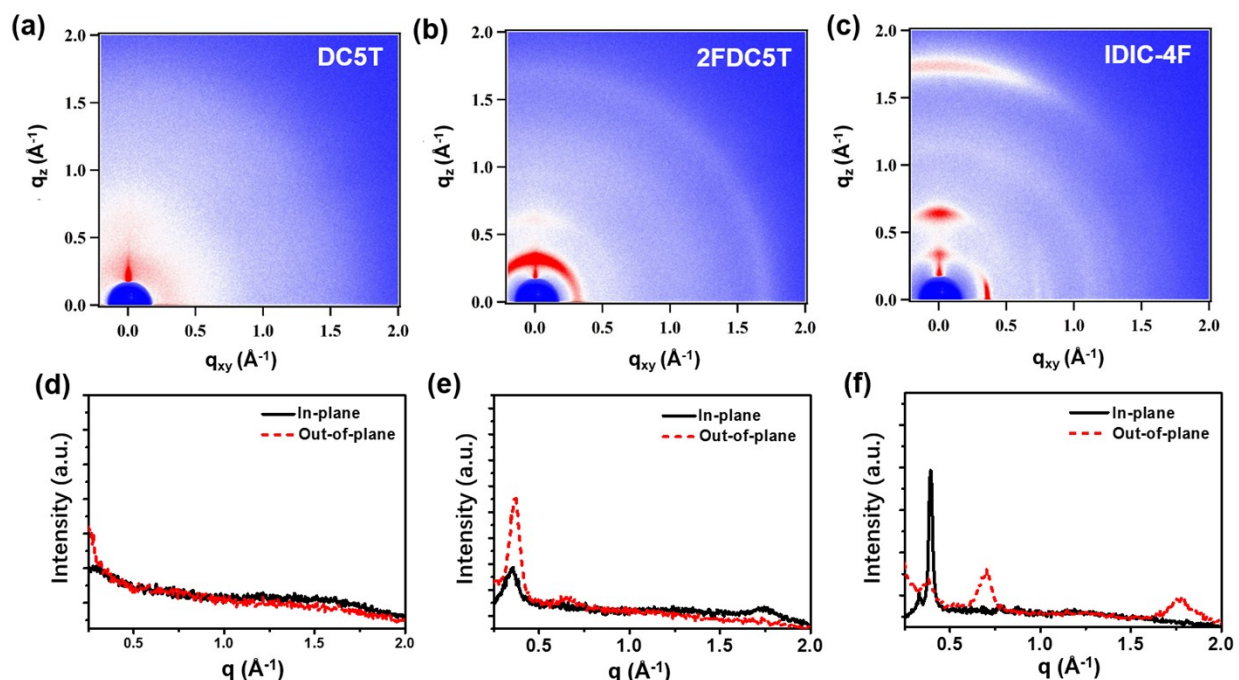


Figure S7. 2D GIWAXS patterns of (a) DC5T:IDIC-4F, (b) 2FDC5T:IDIC-4F and The GIWAXS intensity profiles of (c) DC5T:IDIC-4F, (d) 2FDC5T:IDIC-4F, the in-plane (black solid lines) and out-of-plane (red dashed lines) directions, respectively.

Table S1. In-plane and out-of-plane parameters extracted from the 2D GIWAXS of pristine films.

Component	Peak	Peak location (\AA^{-1})	d-spacing (\AA)	FWHM (\AA^{-1})	Crystal coherence length(nm)
DC5T	(100)IP	0.32	19.62	0.731	0.773
	(010)IP	1.518	4.14	0.909	0.622
	(010)OOP	1.529	4.11	1.022	0.553
2FDC5T	(100)IP	0.36	17.44	0.049	11.4
	(010)IP	1.742	3.61	0.256	2.21
	(100)OOP	0.366	17.15	0.063	8.96
	(010)OOP	1.724	3.64	0.463	1.22
IDIC-4F	(100)IP	0.393	15.98	0.025	23.06
	(100)OOP	0.391	16.06	0.063	9.0
	(010)OOP	1.781	3.53	0.202	2.79

12. Different processing conditions in optimizing PCE

Table S2. Photovoltaic performance of **DC5T** -based solar cells with different thermal anneal temperature and device structure ITO/PEDOT:PSS/active layer/ DPO /Ag.

D/A	Thermal Anneal[°C]	V_{oc} [V]	J_{sc} [mA cm ⁻²]	FF[%]	PCE[%]
1:1	110	0.81	10.49	54.87	4.64
1:1	120	0.84	11.89	62.98	6.29
1:1	130	0.86	12.34	66.25	7.03
1:1	140	0.71	10.59	45.74	3.44

Table S3. Photovoltaic performance of **DC5T**-based solar cells with different D/A ratio and device structure ITO/PEDOT:PSS/active layer/ DPO /Ag.

D/A	Thermal Anneal [°C]	V_{oc} [V]	J_{sc} [mA cm ⁻²]	FF[%]	PCE[%]
1:1	130	0.86	12.34	66.25	7.03
1:1.2	130	0.84	10.39	59.85	5.22
1.2:1	130	0.84	11.27	60.95	5.77
1:1.5	130	0.84	10.60	63.23	5.63
1.5:1	130	0.84	10.76	59.66	5.39

Table S4. Photovoltaic performance of **2FDC5T** -based solar cells with different thermal anneal temperature and D/A ratio temperature and device structure ITO/PEDOT:PSS/active layer/ DPO /Ag.

D/A	Thermal Anneal [°C]	V_{oc} [V]	J_{sc} [mA cm ⁻²]	FF[%]	PCE[%]
1:1	100	0.80	17.39	55.61	7.74
1:1	110	0.93	17.26	54.02	8.67
1:1	130	0.77	15.51	46.90	5.60
1.2:1	110	0.74	14.15	42.71	4.47
1:1.2	110	0.80	15.88	46.77	5.94
1.5:1	110	0.77	14.67	42.15	4.76
1:1.5	110	0.85	15.66	51.23	6.28

Table S5. Photovoltaic performance of **2FDC5T** -based solar cells with different hot substrate temperature and device structure ITO/PEDOT:PSS/active layer/ DPO /Ag.

D/A	Hot Substrate and Thermal Anneal[°C]	V_{oc} [V]	J_{sc} [mA cm ⁻²]	FF[%]	PCE[%]
1:1	30+110	0.92	17.26	54.02	8.67
1:1	45+110	0.92	17.53	54.87	9.02
1:1	55+110	0.90	16.37	51.65	7.53
1:1	65+110	0.91	15.26	48.99	6.80

Table S6.
Photovoltaic performance of **DC5T** -based solar cells with different Solvent Anneal and device structure ITO/PEDOT:PSS/active layer/ DPO /Ag.

D/A	Solvent Anneal	V_{oc} [V]	J_{sc} [mA cm ⁻²]	FF[%]	PCE[%]
1:1	CF	0.77	5.51	22.99	1.22
1:1	CS ₂	0.91	6.08	35.87	1.98
1:1	THF	0.87	5.79	33.01	1.68
1:1	DMDS	0.90	3.95	32.68	1.16
1:1	DCM	0.72	1.55	30.37	0.34

Table S7. Photovoltaic performance of **DC5T** -based solar cells with different solvent additive and device structure ITO/PEDOT:PSS/active layer/ DPO /Ag.

D/A	Solvent Additive	V_{oc} [V]	J_{sc} [mA cm ⁻²]	FF[%]	PCE[%]
1:1	DIO	0.14	-	31.47	-
1:1	DPE	0.13	-	30.17	-
1:1	CN	0.35	0.14	26.82	0.01
1:1	NMP	0.31	-	27.73	-

Table S8. Photovoltaic performance of **2FDC5T** -based solar cells with different Solvent Anneal and device structure ITO/PEDOT:PSS/active layer/ DPO /Ag.

D/A	Solvent Anneal	V_{oc} [V]	J_{sc} [mA cm ⁻²]	FF[%]	PCE[%]
1:1	CF	0.83	15.79	48.02	6.29
1:1	CS ₂	0.82	6.19	27.69	1.51
1:1	THF	0.61	6.09	27.14	1.01
1:1	DMDS	0.78	5.99	26.87	1.26
1:1	DCM	0.80	6.97	27.02	1.51

Table S9. Photovoltaic performance of **2FDC5T** -based solar cells with different solvent additive and device structure ITO/PEDOT:PSS/active layer/ DPO /Ag.

D/A	Solvent Additive	V_{oc} [V]	J_{sc} [mA cm ⁻²]	FF[%]	PCE[%]
1:1	DIO	0.79	7.53	49.03	2.92
1:1	DPE	-	-	-	-
1:1	CN	0.77	5.89	37.63	1.70
1:1	NMP	-	-	-	-

13. Solution NMR Spectra

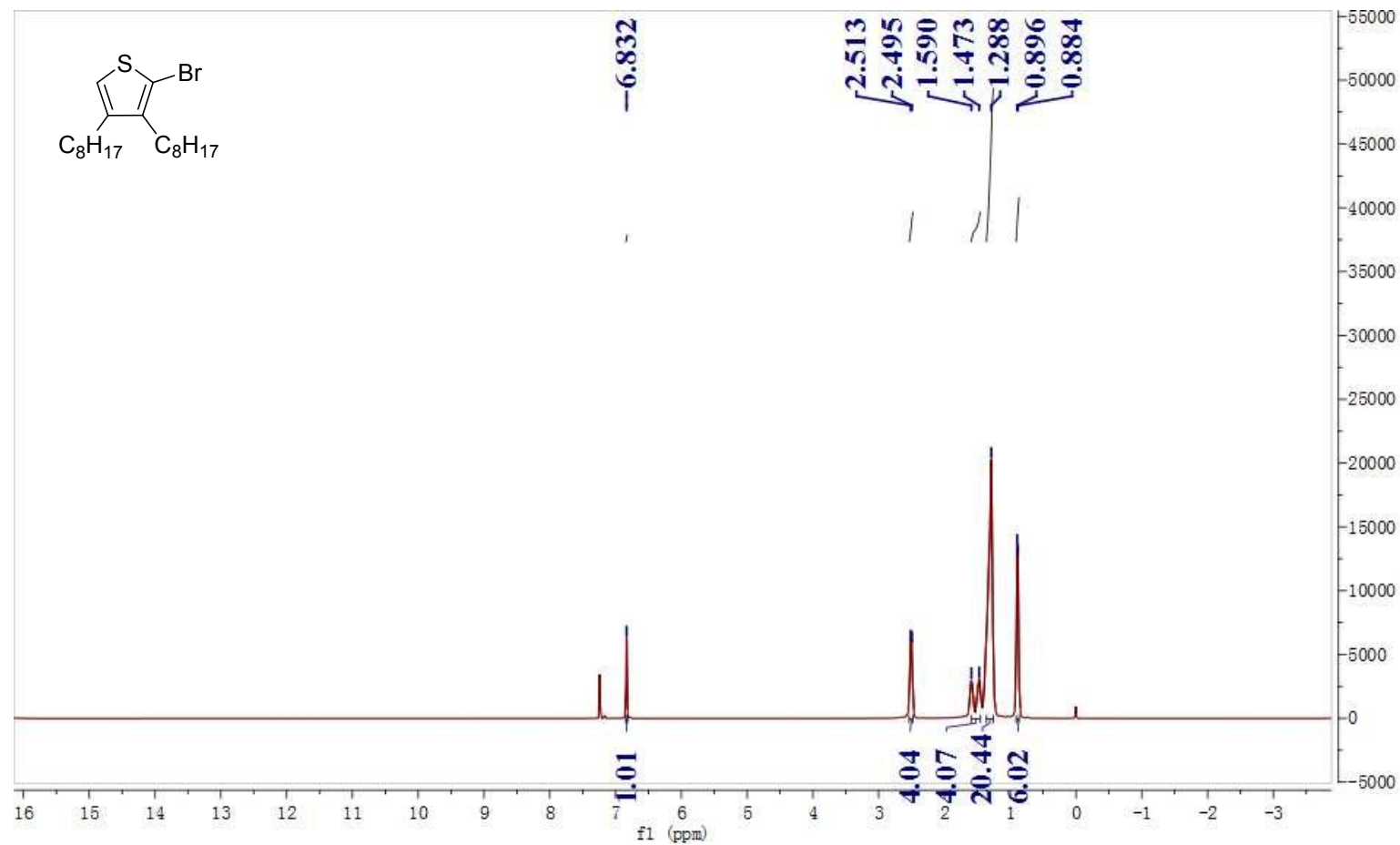


Figure S8. ^1H NMR spectrum of **1** in CDCl_3 .

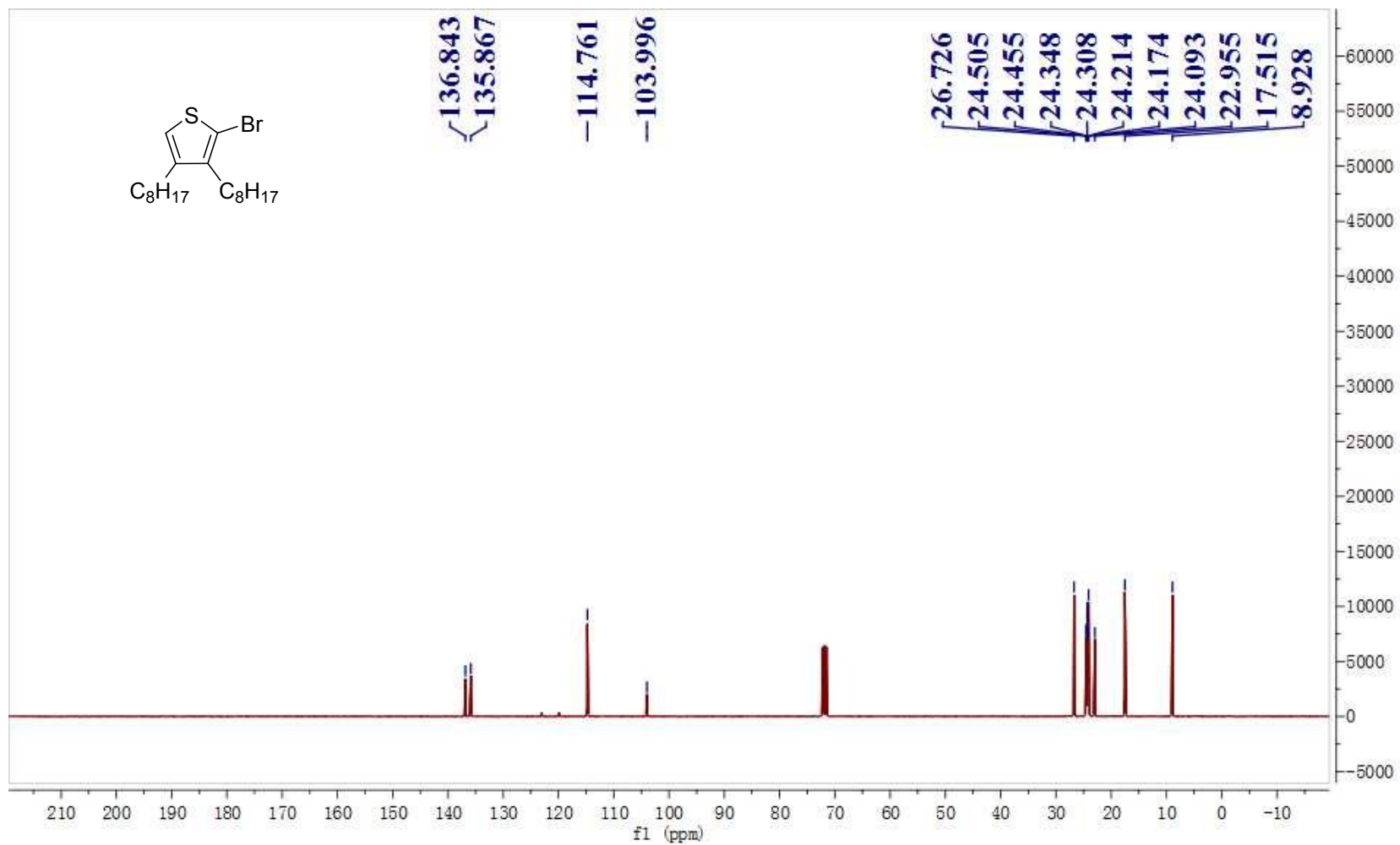


Figure S9. ¹³CNMR spectrum of **1** in CDCl₃.

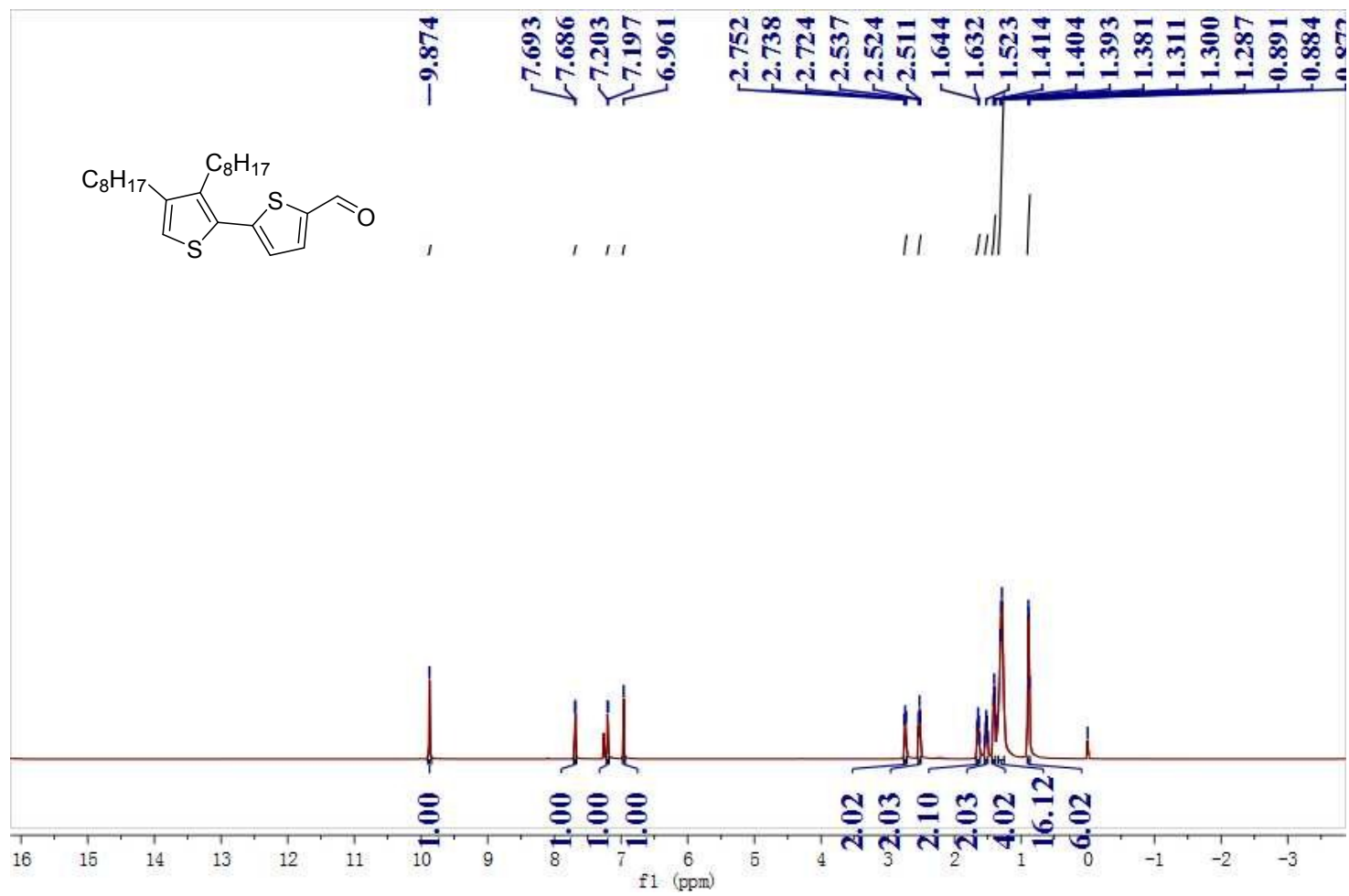


Figure S10. ¹H NMR spectrum of **3** in CDCl₃.

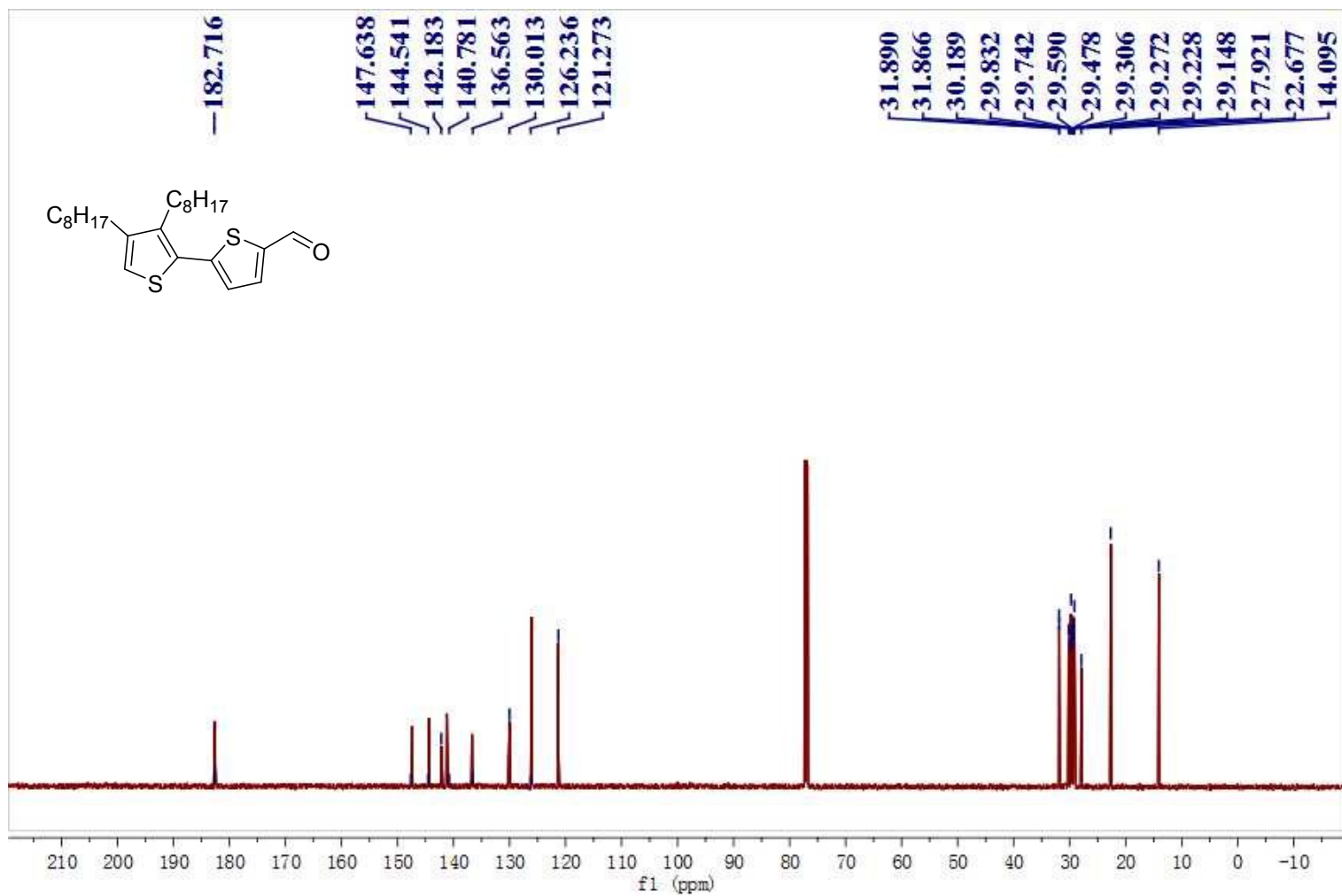


Figure S11. ^{13}C NMR spectrum of **2** in CDCl_3 .

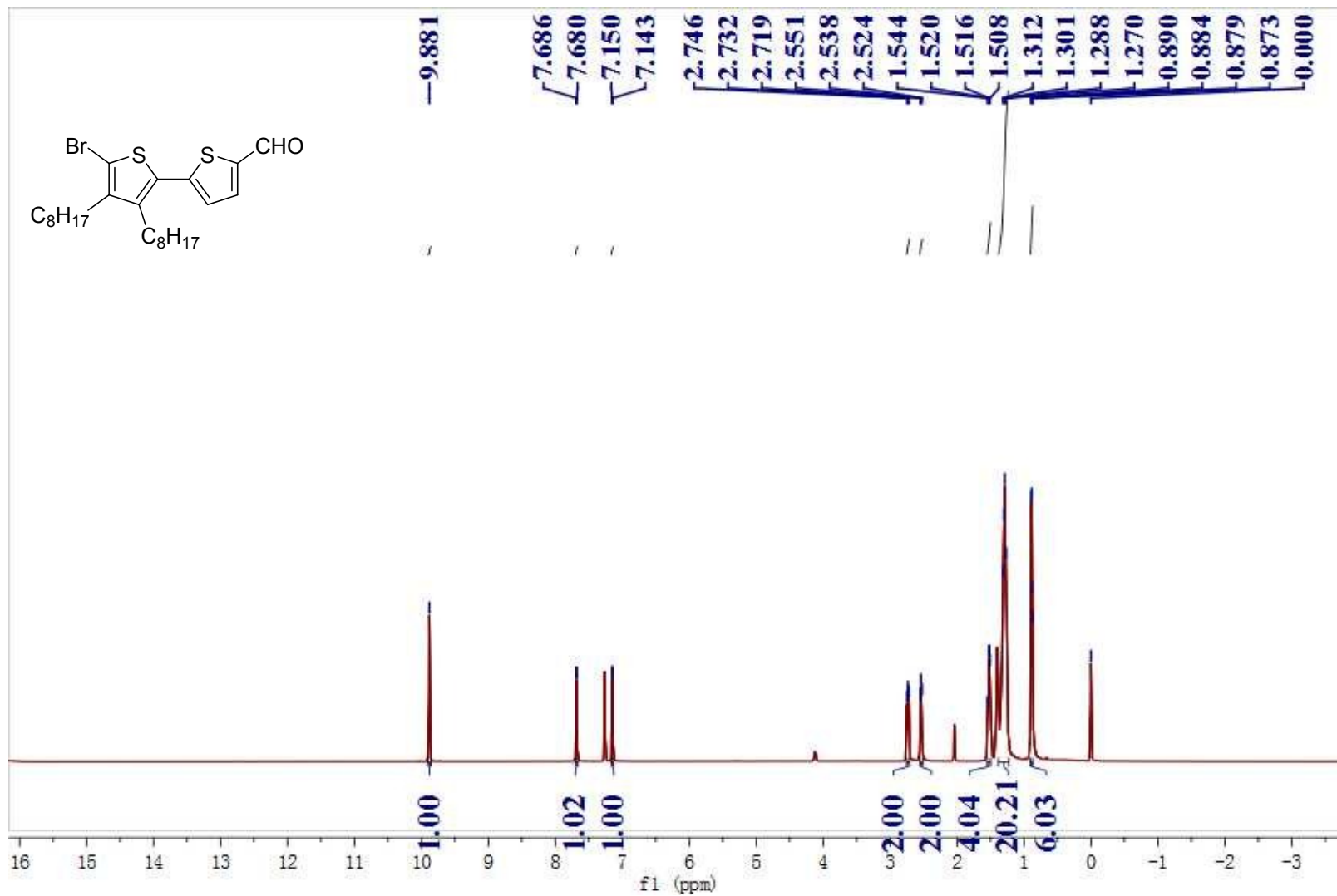


Figure S12. ^1H NMR spectrum of 4 in CDCl_3 .

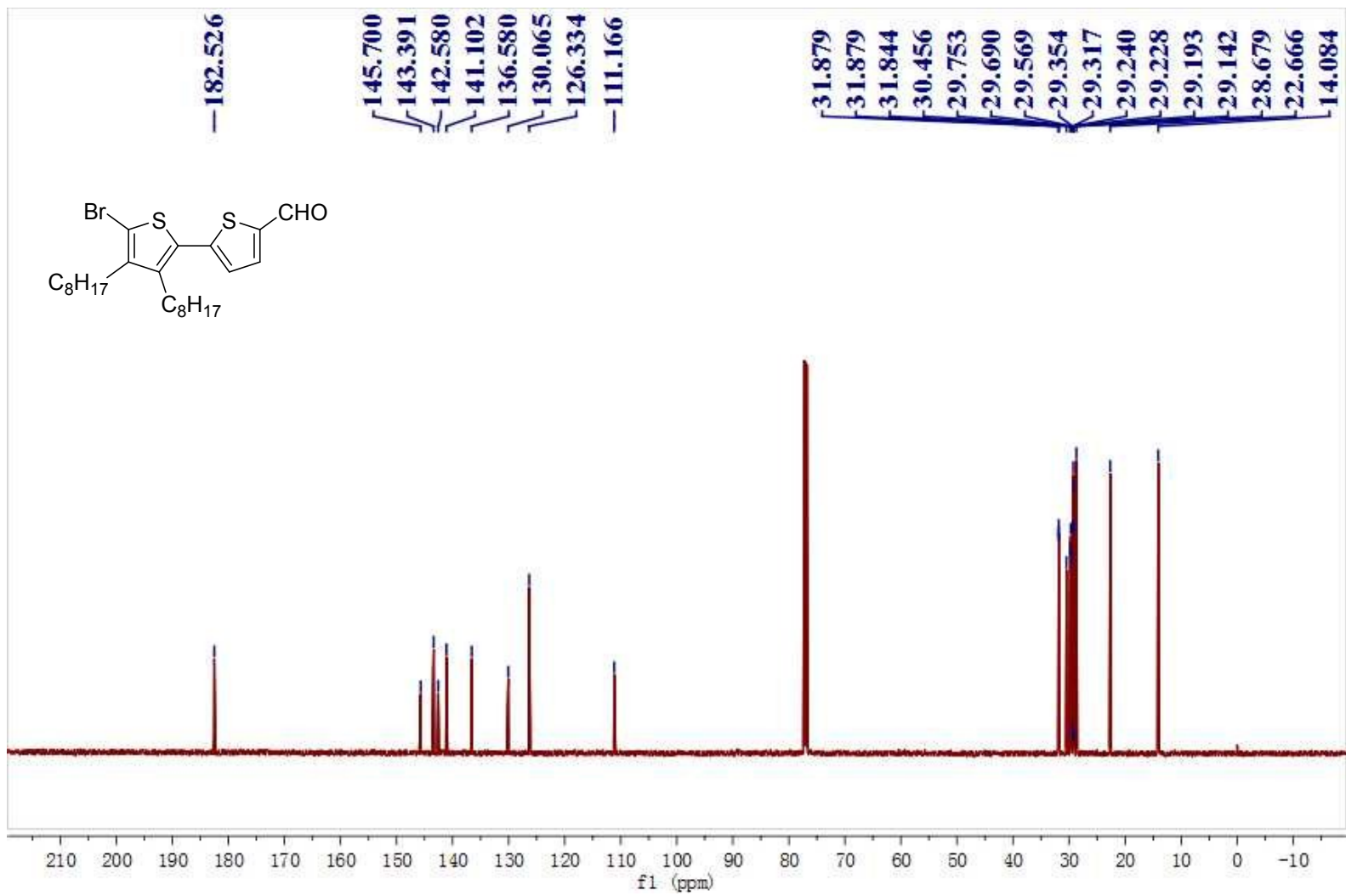


Figure S13. ¹³C NMR spectrum of **4** in CDCl₃.

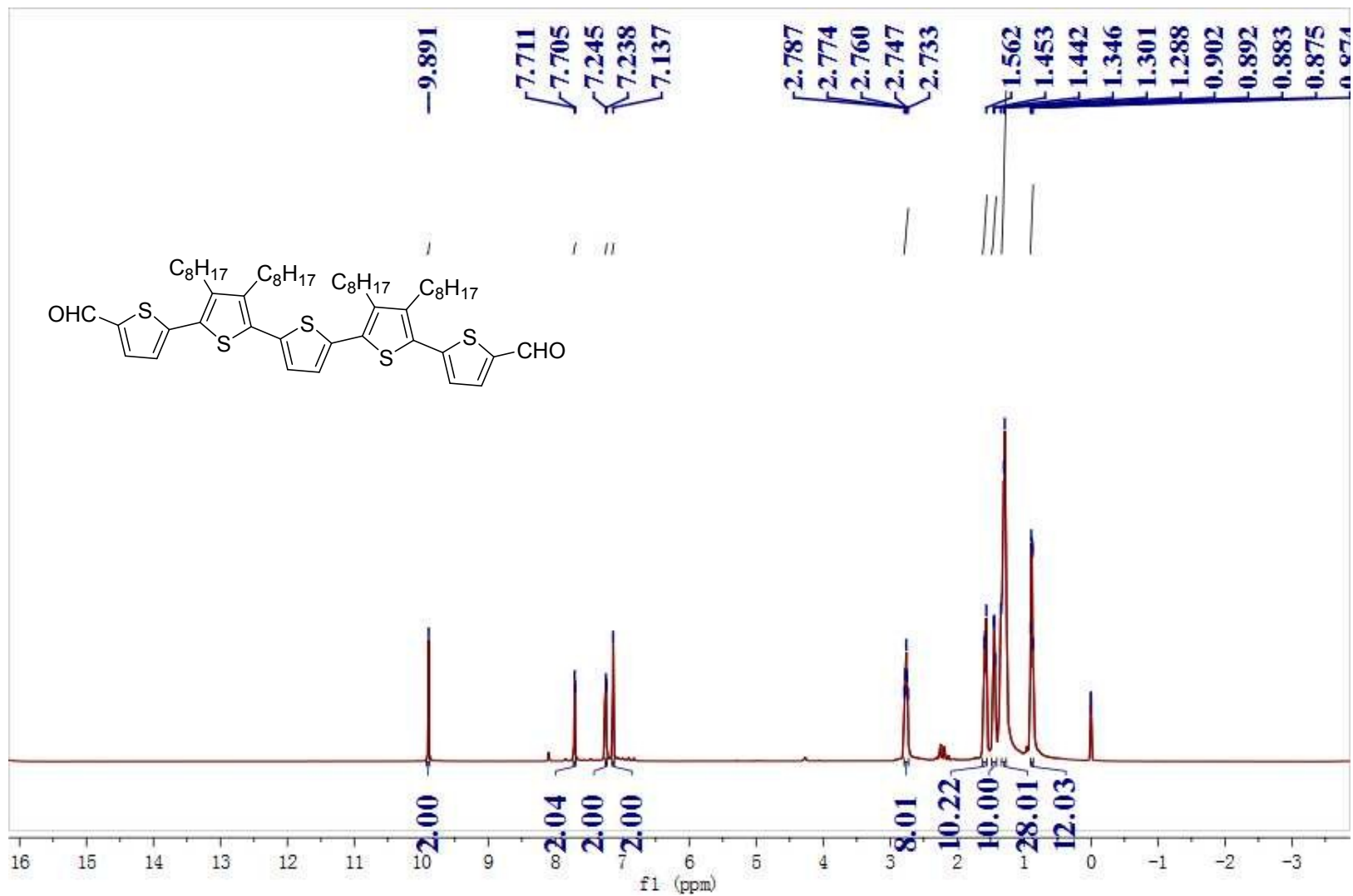


Figure S14. ¹H NMR spectrum of **5** in CDCl₃.

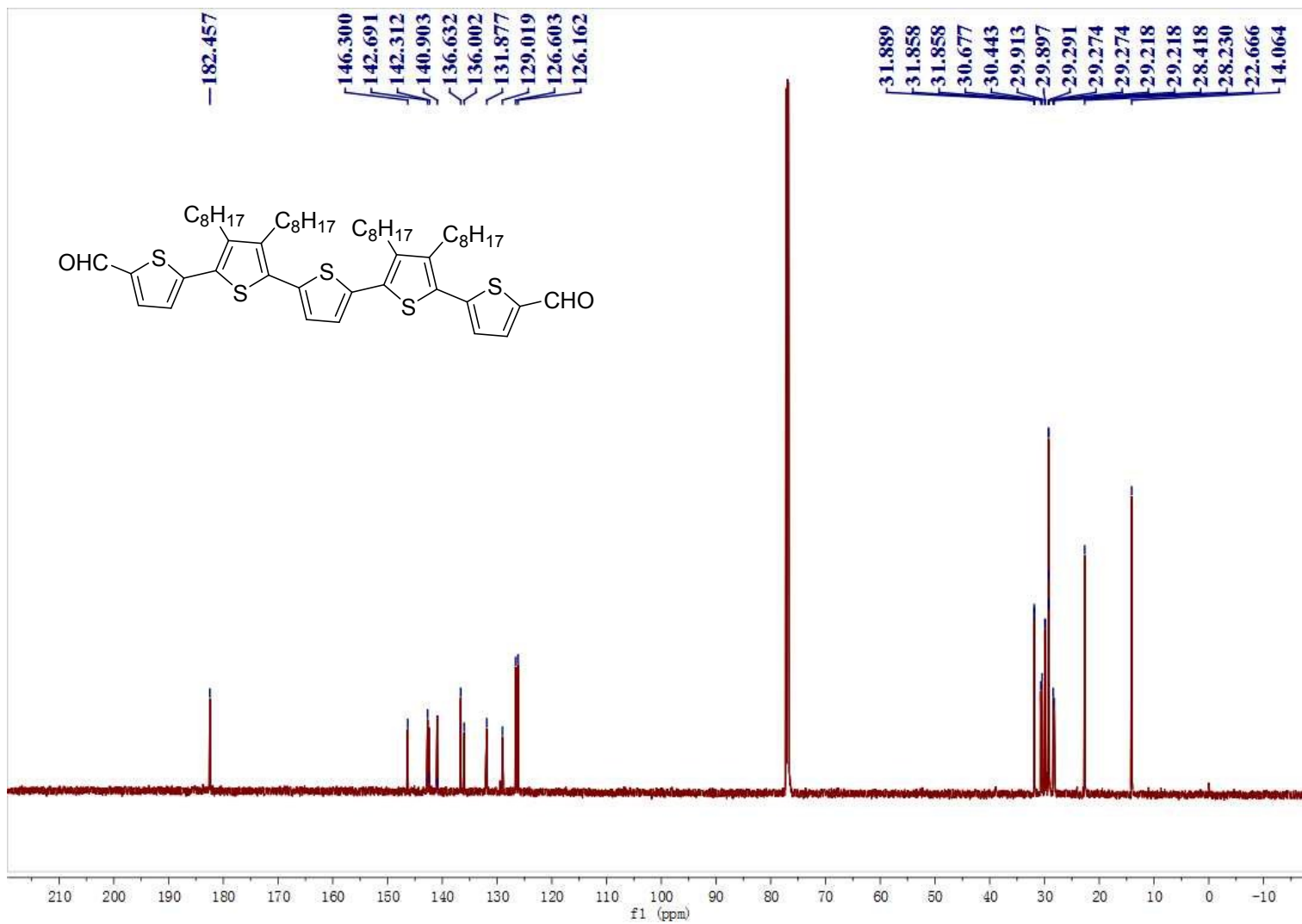


Figure S15. ¹³C NMR spectrum of **5** in CDCl₃.

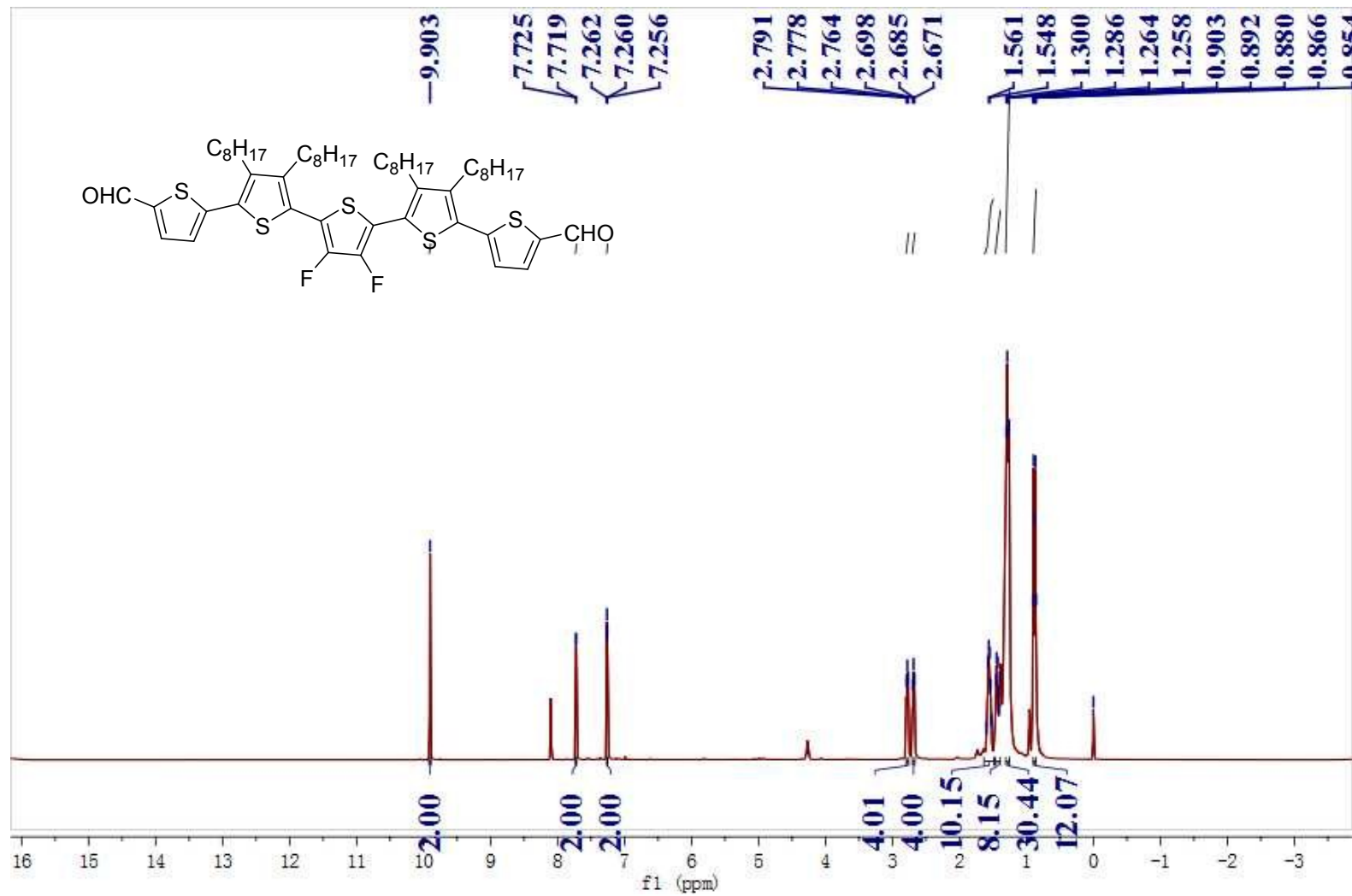


Figure S16. ¹H NMR spectrum of 6 in CDCl₃.

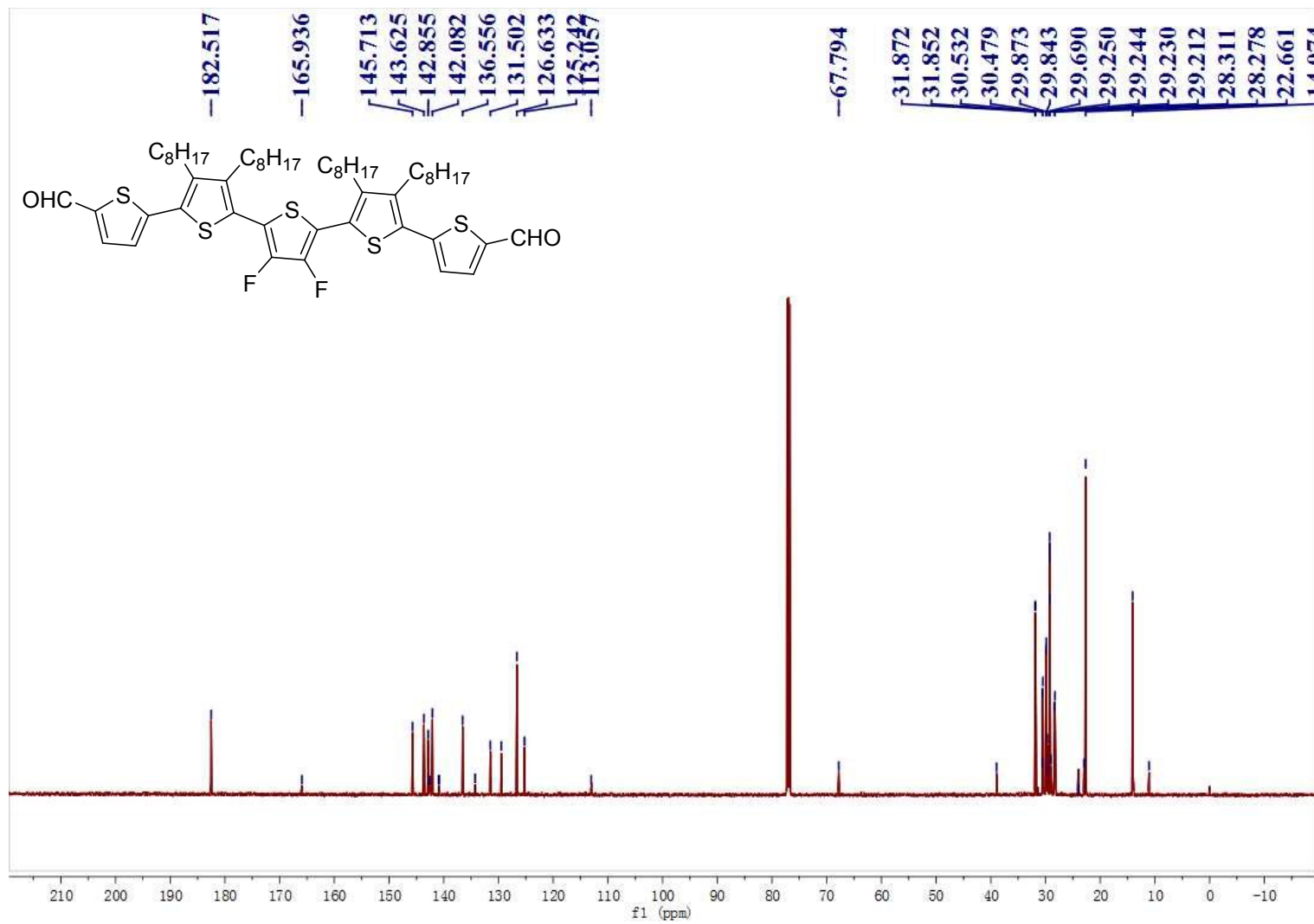


Figure S17. ¹³CNMR spectrum of 6 in CDCl₃.

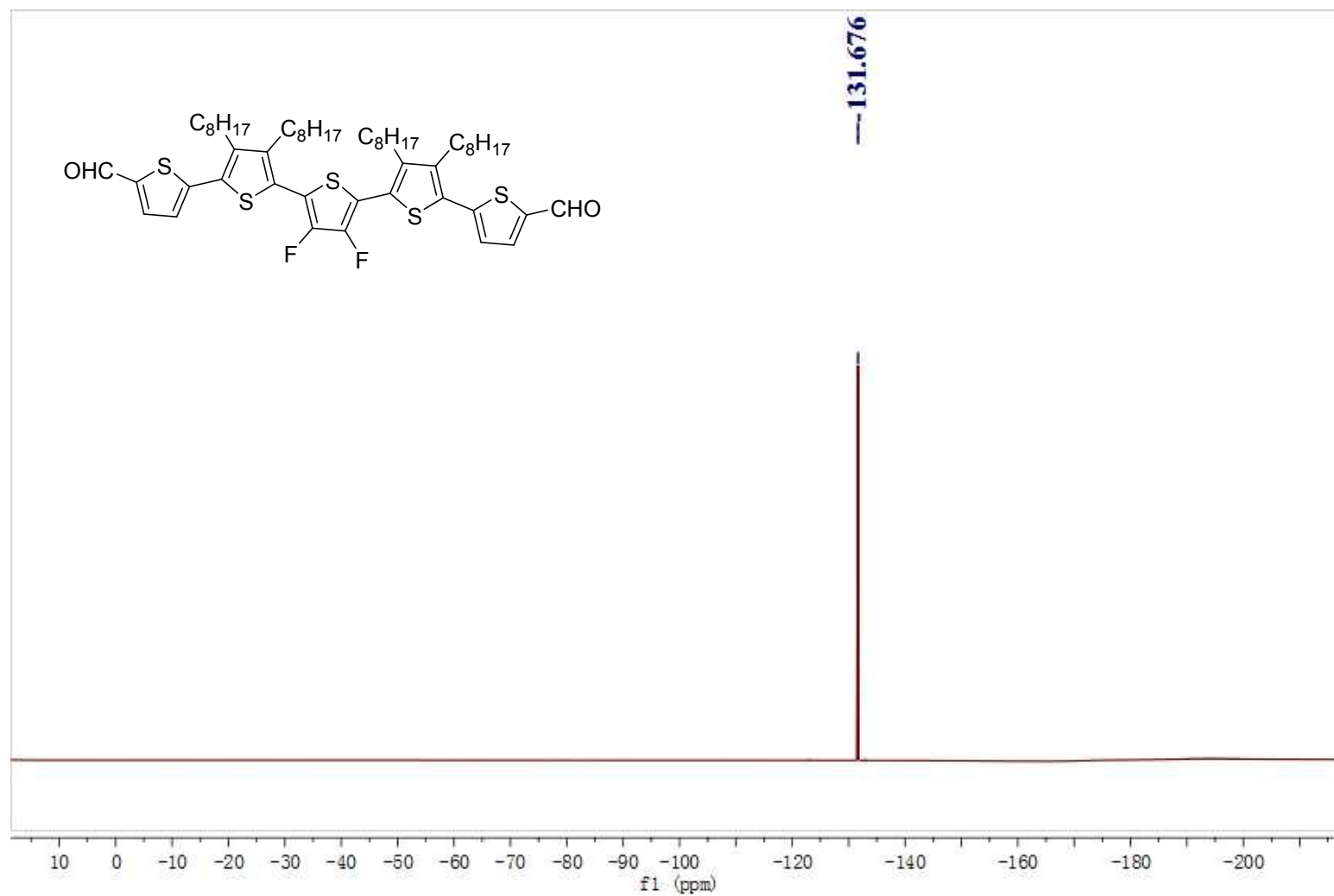


Figure S18. ^{19}F NMR spectrum of **6** in CDCl_3 .

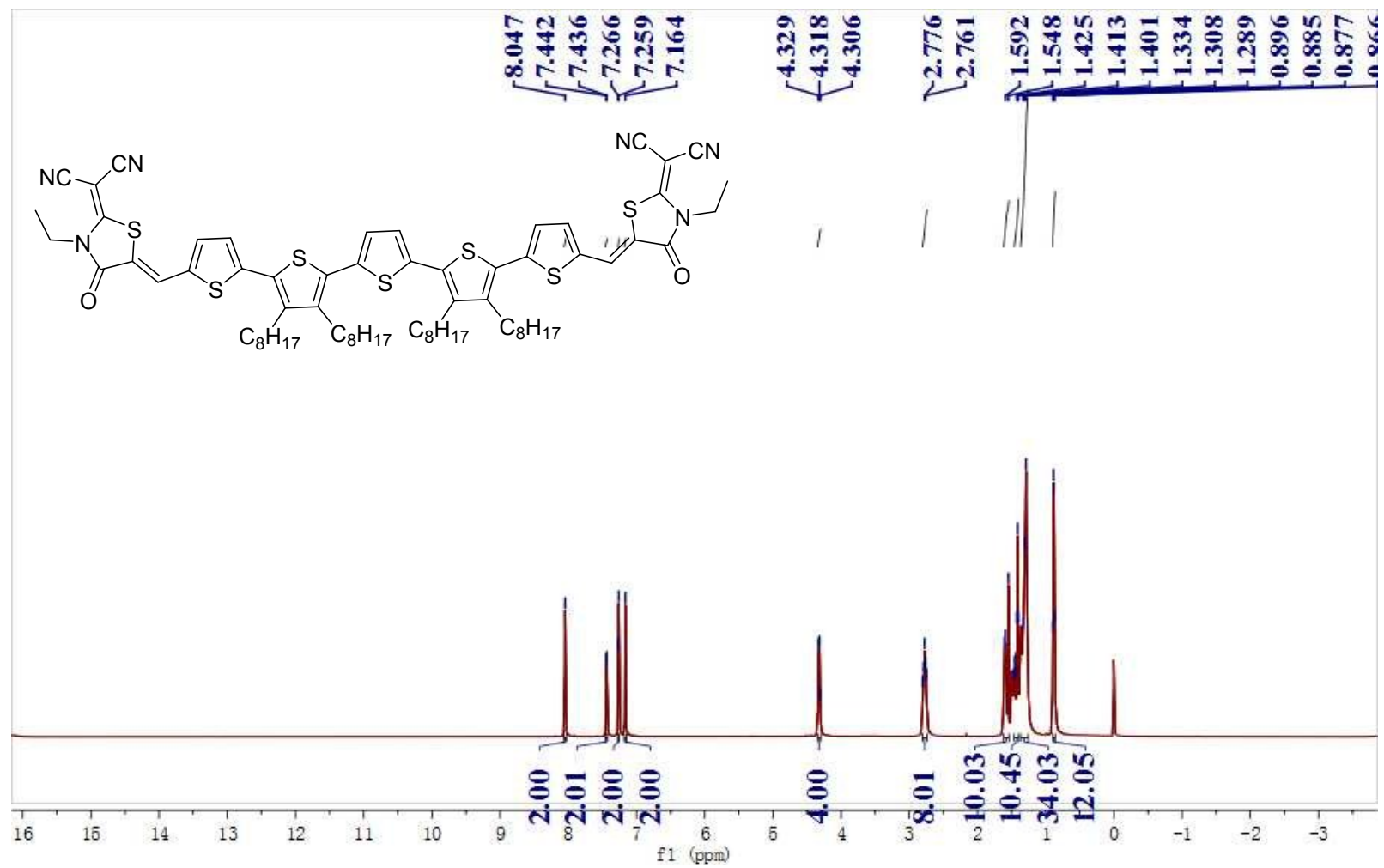


Figure S19. ^1H NMR spectrum of DC5T in CDCl_3 .

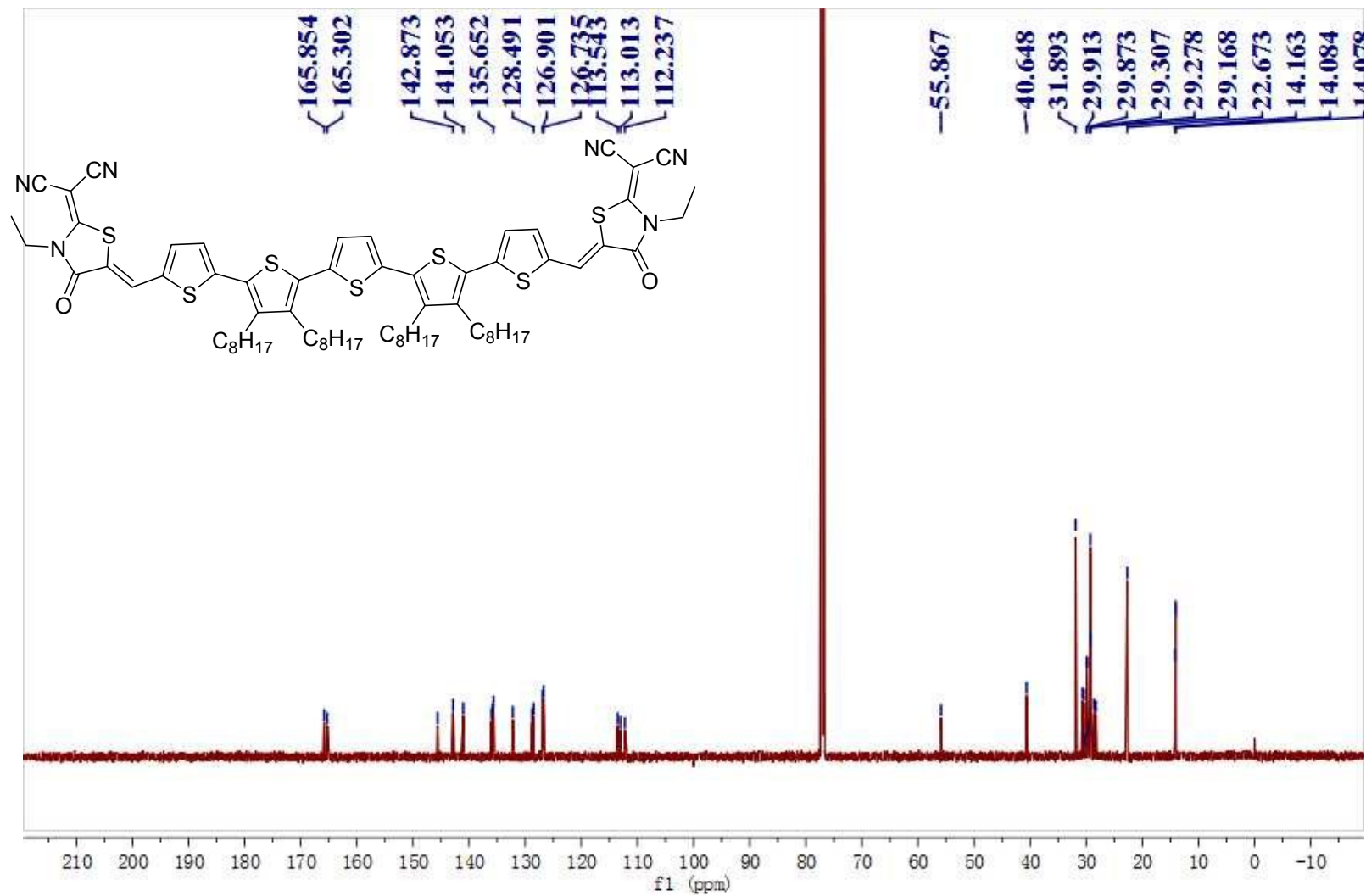


Figure S20. ¹³C NMR spectrum of DC5T in CDCl₃.

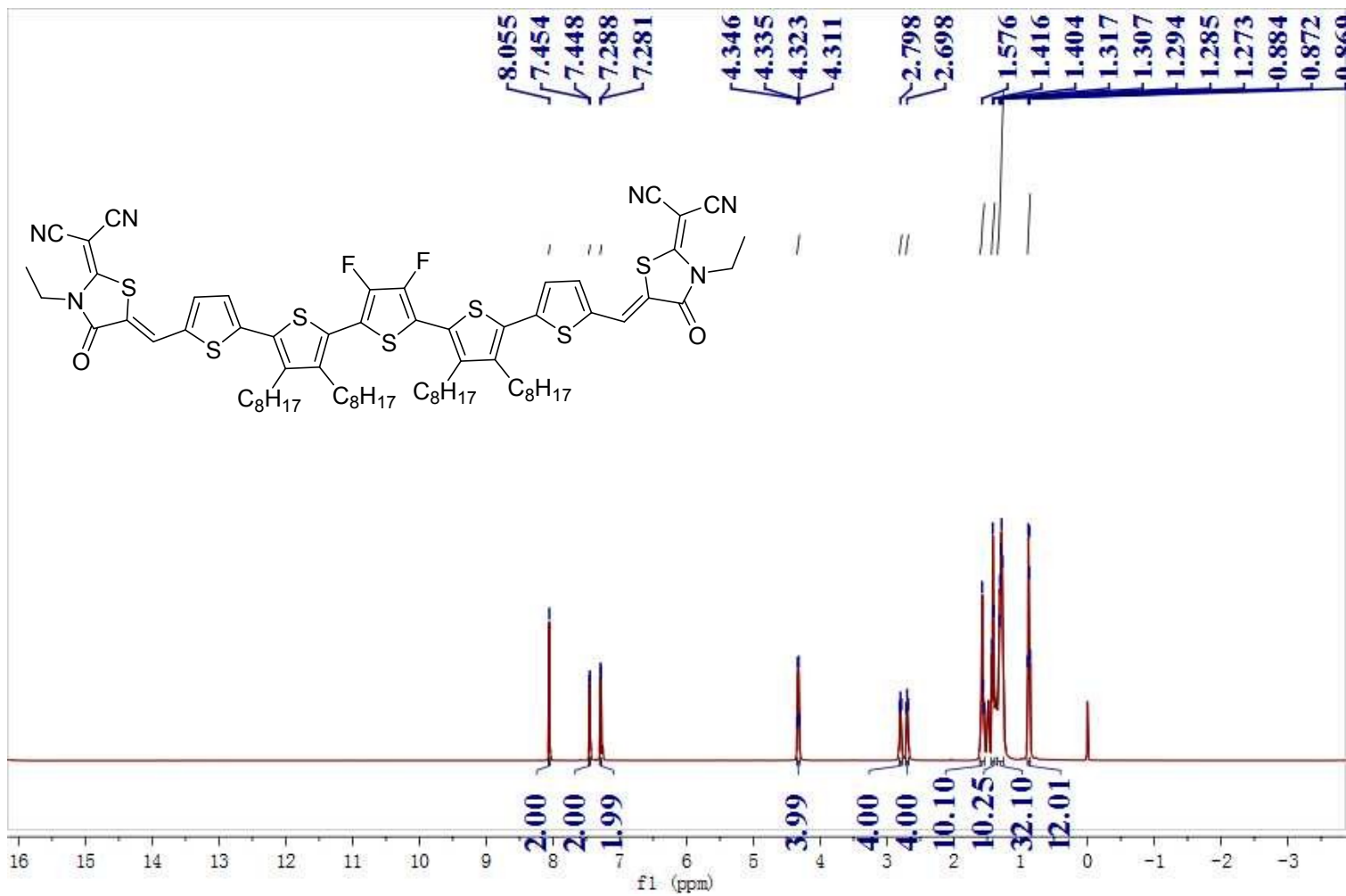


Figure S21. ¹H NMR spectrum of 2FDC5T in CDCl₃.

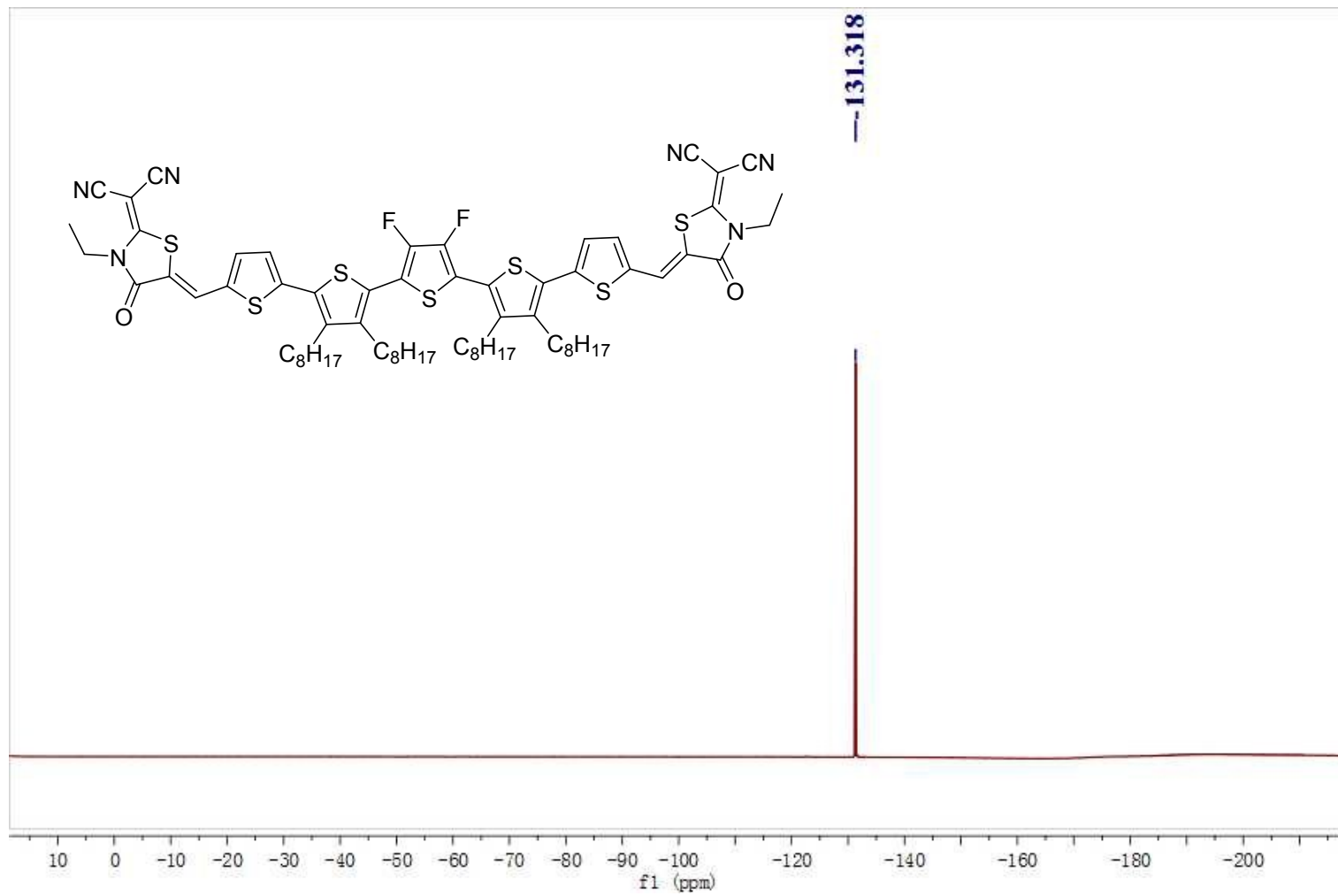


Figure S23. ^{19}F NMR spectrum of **2FDC5T** in CDCl_3 .

14. References

- [1]. S. Ko, E. Verploegen, S. Hong, R. Mondal, E. T. Hoke, M. F. Toney, M. D. McGehee and Z. Bao, *J. Am. Chem. Soc.*, 2011, **133**, 16722-16725.